# The influence of microchemistry on the recrystallization texture of cold-rolled Al-Mn-Fe-Si alloys



2015 IOP Conf. Ser.: Mater. Sci. Eng. 82 012035

(http://iopscience.iop.org/1757-899X/82/1/012035)

# The influence of microchemistry on the recrystallization texture of cold-rolled Al-Mn-Fe-Si alloys

**K Huang[1*], YJ Li[1] and K Marthinsen[1]**

[1] Department of Materials Science and Engineering, Norwegian University of Science and Technology, Trondheim, N-7491 Trondheim, Norway

[*] E-mail: ke.huang@ntnu.no, huangke0729@hotmail.com

**Abstract.** The recrystallization textures of a cold-rolled Al-Mn-Fe-Si model alloy with three different microchemistry states after non-isothermal annealing were studied. The microstructure and texture evolution have been characterized by EBSD. It is clearly demonstrated that the actual microchemistry state as determined by the homogenization procedure strongly influence the recrystallized grain size and recrystallization texture after non-isothermal annealing. High Mn content in solid solution promotes stronger concurrent precipitation and retards recrystallization, which finally leads to a coarse grain structure, accompanied by strong P {011}<566> and/or M {113}<110> texture components and a ND-rotated cube {001}<310> component. A refined grain structure with Cube {001}<100> and/or a weak P component as the main texture components were obtained when the pre-existing dispersoids are coarser and fewer, and concurrent precipitation is limited. The different recrystallization textures are discussed with respect to the effect of second-phase particles using two different heating rates.

## 1. Introduction

The recrystallization texture of cold rolled aluminium alloys after annealing has been the subject of numerous investigations as part of a general effort to optimize their mechanical properties. Different from high purity aluminium alloys, almost all commercial aluminium alloys are multiphase, containing second-phase particles formed either before or during annealing. Considering Al-Mn-Fe-Si (AA3xxx) alloys, the supersaturated Mn in solid solution in the as-cast state will precipitate as Mn-bearing dispersoids during subsequent thermo-mechanical processing steps. The particles may affect the recrystallization texture in different ways. Coarse pre-existing constituent particles favour Particle Stimulated Nucleation (PSN) associated with a wide range of nucleus orientations, and thus yields an overall random recrystallization texture [1,2]. On the other hand, fine dispersoids especially those precipitated during annealing may pin boundaries leading to an elongated coarse grain structure [3] together with the P and ND-rotated cube texture components [4]. The microchemistry state of the alloys, i.e. amount of solutes and second-phase particle structures, determined by the chemical composition and homogenization procedures of the alloys is thus an important aspect in studying the recrystallization textures of cold-rolled Al-Mn-Fe-Si alloys. The recrystallization texture after isothermal annealing of various deformed aluminium alloys has been extensively investigated [3,4]. Much less studies on recrystallization texture after non-isothermal heat treatments exist, which are frequently carried out during industrial thermo-mechanical processing where extended recovery and precipitation of dispersoids are likely to occur, producing complex interactions with recrystallization.

In this paper, the effect of microchemistry on the recrystallization texture of cold-rolled Al-Mn-Fe-Si alloys is analysed after non-isothermal annealing. The different recrystallization

textures obtained are discussed with respect to the second-phase particle structures, including pre-existing dispersoids and concurrently precipitated dispersoids.

## 2. Experimental

The starting material was a DC-cast AA3xxx extrusion billet, supplied by Hydro Aluminium. The chemical composition (wt.%) is 0.152% Si, 0.530% Fe, 0.390% Mn with the balance Al. The detailed description of the as-cast material can be found in Ref [5,6]. The as-cast material (C1-0) was subsequently homogenized at two different conditions to get different amounts of Mn in solid solution and dispersoid densities. One set of samples were heated with a heating rate of 50 $^{o}$C /h to 450 $^{o}$C and kept for 4 hours, referred to as C1-2, to be consistent with previous work on the same set of alloys [6-8]. Another set of samples were subjected to a two-stage homogenization treatment. The samples were first heated at 50$^{o}$C/h to 600 $^{o}$C for 4 hours, and then cooled at 25 $^{o}$C /h to 500$^{o}$C where they were kept for another 4 hours, which gave the C1-3 condition. Materials were water quenched to room temperature at the end of the homogenization procedure. Characteristics of the three microchemistry variants are listed in Table 1, while example images of their typical size and distribution can be found in Ref [6]. From Table 1, it is clear that the as-cast variant C1-0 has the highest potential for concurrent precipitation, while the C1-2 variant possesses a high density of fine pre-existing dispersoids. The homogenized samples were cold rolled at room temperature in multiple passes to a deformation strain of $\varepsilon$ = 3.0. The rolled sheets were then non-isothermally annealed in an air circulation furnace to a target temperature, and then held for $10^5$s at that temperature before water quench. The heating rate during non-isothermal annealing was 100°C/h and 200°C/h, respectively. The microstructure characterization details have been presented elsewhere [6].

Table 1 Electrical conductivity, solute (Mn) concentrations, equivalent area diameter and number density of particles in the alloys studied [6]

| | Electrical conductivity (m/Ωmm$^2$) | Concentration of Mn (wt%) | Constituent particles | | Dispersoids | |
|---|---|---|---|---|---|---|
| | | | Diameter (μm) | Number density (mm$^{-2}$) | Diameter (μm) | Number density (mm$^{-2}$) |
| C1-0 | 23.9 | 0.35 | 0.88 | 2.8e4 | - | - |
| C1-2 | 27.5 | 0.16 | 0.96 | 2.9e4 | 0.054 | 1.3e6 |
| C1-3 | 29.0 | 0.11 | 1.10 | 2.1e4 | 0.127 | 5.5e4 |

## 3. Results and discussion

The first set of results refers to the heating rate of 100°C/h to a target temperature of 400°C. The recrystallization textures of all three variants were characterized by EBSD and are presented in Fig.1. For the as-cast variant C1-0, which has the highest potential for concurrent precipitation (see Table 1), strong P and M {113}<110> texture components, together with a medium strength 35° ND-rotated cube component are obtained. For C1-2, the recrystallization texture is characterized by a very sharp P texture component and a 22° ND-rotated cube component. A much weaker P texture is obtained for C1-3, while a strong cube texture component is observed together with a medium strength S {123}<634> texture component, which is very weak for the other two variants. The weak P texture for C1-3 suggests that the strength of the P component is related to concurrent precipitation and/or

pre-existing disperoids. The intensity of the P texture component was found to increase with the initial amount of Mn content during isothermal annealing [4]. The reason why C1-2 (which has less Mn in solid solution than C1-0) has the strongest P texture in the present case is related to the temperature at which it was recrystallized, an aspect which will be discussed in detail in a separate paper. When decreasing the amount of Mn in solid solution, a transition from 35° ND-rotated cube to 22° ND-rotated cube and finally to pure cube was found. In terms of recrystallized grain size, a coarse recrystallized grain structure was obtained for C1-0 and C1-2, while C1-3 exhibits a more refined grain structure, further confirming the latter being less affected by concurrent precipitation and pre-existing dispersoids, as shown in Table 2. The microstructure of the three variants, in terms of typical EBSD micrographs can be found in Ref [5].

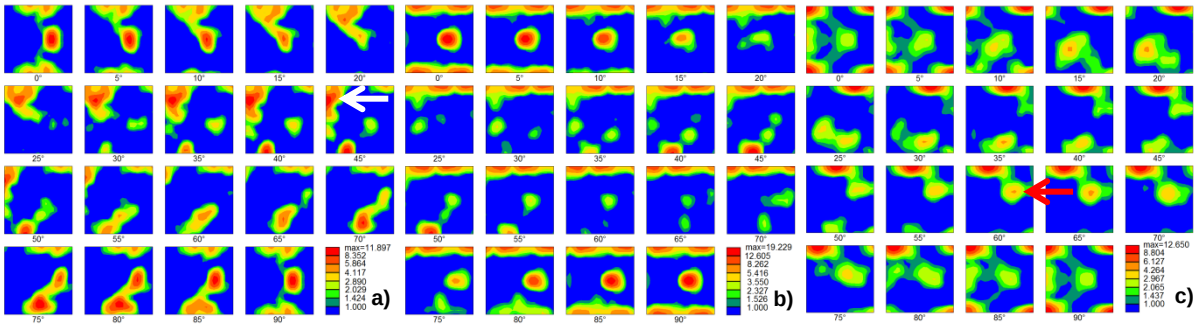


Fig. 1 ODF maps showing the textures of the three variants after heating at 100°C/h to 400 °C and kept for $10^5$s. The M and S texture components are pointed out by white and red arrow, respectively
a) C1-0， b) C1-2， C) C1-3

Table 2 Effect of microchemistry on the recrystallized grain size after annealing at different heating rates to 400°C and kept for $10^5$s

| | Grain size (μm) | | |
|---|---|---|---|
| | C1-0 | C1-2 | C1-3 |
| 100°C/h | 157 | 157 | 49 |
| 200°C/h | 117 | 131 | 34 |

In general, increasing the heating rate to 200°C/h tends to weaken the recrystallization textures, as shown in Fig.2. The variation of texture components with microchemistry, however, exhibits the same tendency as the cases annealed with the slower heating rate. With higher heating rate, there is less interaction time between recrystallization and concurrent precipitation, which is the main reason a weaker P texture were obtained with the higher heating rate. For C1-3, when the heating rate was increased from 100°C/h to 200°C/h, the intensity of cube texture decreased slightly, from 12x random to 8x random. This is related to the fact that recrystallization started at a higher temperature for the former case, due to stronger recovery and concurrent precipitation. It is reported that increasing annealing temperature enhances the strength of the cube texture for this material [6]. On the other side, the intensity of the P texture weakens at higher annealing temperatures due to fast recrystallization kinetics and less interaction with concurrent precipitation, the activation of other possible nucleation sites (grain boundaries, other deformation heterogeneities, etc.) might also have played a role [6,9]. As shown in Table 2, the recrystallized grain sizes for the three variants heated at 200°C/h are obviously smaller than their counterparts annealed at the lower heating rate of 100°C/h, again with the most refined grain structure obtained by the C1-3 variant where both concurrent precipitation and pre-existing particles are limited.

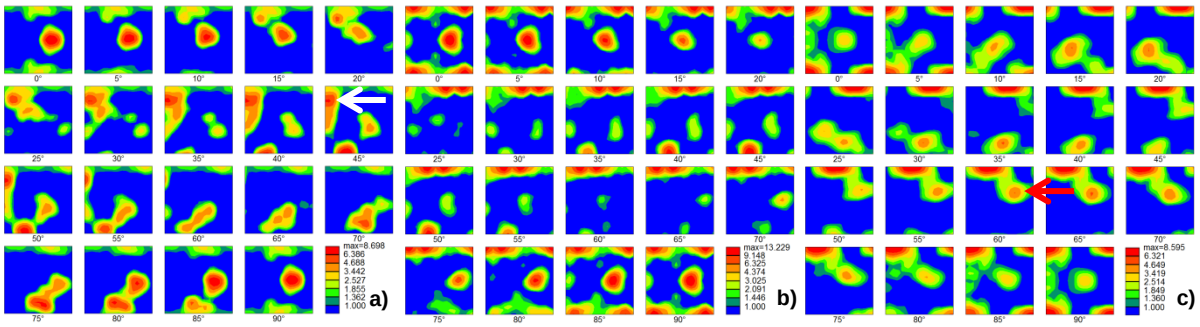


Fig. 2 ODF maps showing the textures of the three variants after heating at 200°C/h to 400°C and kept for $10^5$s, where the M and S texture components are pointed out by white and red arrow, respectively.
a) C1-0， b) C1-2， C) C1-3

From the above analyses, different microchemistry states, as obtained after different homogenizations of the same alloy, have proved to significantly affect the recrystallization textures. It is hard, however, to distinguish and quantify how pre-existing dispersoids and concurrent precipitation affect the nucleation and growth behaviour. Further investigations focusing on the origin and evolution of different texture components need to be done to clarify this aspect [10]. Physically based numerical models [e.g.11,12] which take into account the interaction between recrystallization and second-phase particles may also be helpful to obtain a better understanding of this complicated interaction.

## 4. Conclusions

The microstructural evolution of an Al-Mn-Fe-Si alloy during annealing after cold rolling has been investigated. Specifically, the effect of microchemistry state, in terms of amount of Mn in solid solution, constituents, size and number density of dispersoids, introduced prior to cold rolling, through different homogenization treatments, on recrystallization texture has been analysed after non-isothermal heating experiments. It is clearly demonstrated that the microchemistry state strongly affects both the type of recrystallization texture components obtained and their strength. In general, high Mn content in solid solution promotes stronger concurrent precipitation and retards recrystallization, which finally leads to a coarse grain structure, accompanied by strong P and/or M texture components and a ND-rotated cube component. A refined grain structure with Cube and/or a weak P component as the main texture components were obtained when the pre-existing dispersoids are coarser and fewer, and concurrent precipitation is limited.

## Acknowledgements

This research work has been supported by the KMB project (193179/I40) in Norway. The financial support by the Research Council of Norway and the industrial partners, Hydro Aluminium and Sapa Technology is gratefully acknowledged. KH acknowledges the financial support from NTNU through the Strategic Area Materials.

## References

[1] Lücke K and Engler O 1990 Mater. Sci. Technol. 6 1113
[2] Vatne HE, Engler O and Nes E 1997 Mater. Sci. Technol. 13 93
[3] Somerday M and Humphreys FJ 2003 Mater.Sci.Technol. 19 20
[4] Tangen S, Sjølstad K, Furu T and Nes E 2010 Metall. Mater.Trans. A 41A 2970
[5] Huang K, Li YJ and Marthinsen K 2014 Mater. Sci. Forum 783-786 174
[6] Huang K, Wang N, Li YJ and Marthinsen K 2014 Mater.Sci.Eng. A 601 86
[7] Huang K, Li YJ and Marthinsen K 2014 Mater. Sci. Forum 793-796 1163
[8] Huang K, Li YJ and Marthinsen K 2014 Trans. Nonferrous Met. Soc. China 24 3840
[8] Liu WC, Li Z and Man C-S 2008 Mater.Sci.Eng. A 478 173
[9] Schäfer C and Gottstein G 2011 Int. J. Mater. Res. 102 1106
[10] Hersent E, Huang K, Friis J and Marthinsen K 2013 Mater.Sci.Forum.753 143
[11] Schäfer C, Song J and Gottstein G 2011Acta Mater. 57 1026